Context Curves for Classification of Lung Nodule Images

Fan Zhang*, Yang Song*, Weidong Cai*, Yun Zhou†, Shimin Shan‡ and Dagan Feng*
*BMIT Research Group, School of IT, University of Sydney, Australia
†The Russell H. Morgan Department of Radiology and Radiological Science
Johns Hopkins University School of Medicine, Baltimore, USA
‡School of Software, Dalian University of Technology, China
*{fzha8048, yson1723}@uni.sydney.edu.au, *{tom.cai, dagan.feng}@sydney.edu.au, †yunzhou@jhmi.edu, ‡ssm@dlut.edu.cn

***Abstract*—In this paper, a feature-based imaging classification method is presented to classify the lung nodules in low dose computed tomography (LDCT) slides into four categories: *well-circumscribed*, *vascularized*, *juxta-pleural* and *pleural-tail*. The proposed method focuses on the feature design, which describes both lung nodule and surrounding context information, and contains two main stages: (1) superpixel labeling, which labels the pixels into foreground and background based on an image patch division approach, (2) context curve calculation, which transfers the superpixel labeling result into feature vector. While the first stage preprocesses the image, extracting the major context anatomical structures for each type of nodules, the context curve provides a discriminative description for intra- and inter-type nodules. The evaluation is conducted on a publicly available dataset and the results indicate the promising performance of the proposed method on lung nodule classification.**

***Keywords*—lung nodule; feature design; context curve; classification;**

I. Introduction

Lung cancer is the most common malignancy leading to the cancer related death, whose survival is highly dependent on the early and accurate diagnosis [1]. In the past several decades, numerous efforts have been conducted to study the indications of lung cancer from various symptoms of lung-related diseases. Among them, although most of lung nodules have benign causes, many of them represent lung cancers, with nearly 20%-30% of patients with lung cancer initially diagnosed with lung nodule [2]. Therefore, the initial evaluation of the suspected lung nodules, which is to differentiate benign to malignant ones, is important for the early detection of lung cancer.

Lung nodule is the lung tissue abnormality that is roughly spherical with round opacity [3]. Normally, the intra-parenchymal nodules that solitarily locate in the central of lung tend to be more malignant than those connected to the surrounding anatomical structures, such as vessels and pleurae [4]. Thus, according to its relative positions regarding to the these structures, lung nodule is usually categorized into four different types [5], including: well-circumscribed (W), vascularized (V), juxta-pleural (J) and pleural-tail (P). Well-circumscribed nodule is located solitarily in the lung without any connection to other structures. Vascularized nodule has significant connections to its neighbouring vessels. Juxta-pleural nodule is near the pleural surface and has a large portion attached to the pleura. Pleural-tail nodule is also around the pleural surface but only connected to the pleura with a thin tail. Fig.1 shows the sample images for the four stated types of nodules.

This work was supported in part by the ARC grants.

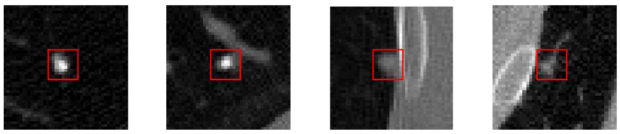

Fig. 1. Sample images from the four categories with well-circumscribed, vascularized, juxta-pleural and pleural-tail cases from left to right respectively. The nodules are located centrally, encircled in red rectangles.

Computer-aided diagnosis (CAD) systems, with the advancements in computed tomography (CT) that enables visualization of small and low-contrast nodules [6], offer a considerable opportunity in classifying various lung nodules automatically. The automated classification is highly useful for facilitating large-scale screening and providing second opinions for radiologists due to the fact that the direct manual interpretation would sometimes be error-prone [7][8]. Therefore, the aim of this work is to provide an automated classification method to categorize various lung nodules into the above four types.

A. Related work

Image classification in medical or general imaging normally contains two major components: feature extraction and classification. Many different classifiers from machine learning area have been involved and proved to be effective in image classification, such as *k*-nearest neighbour (*k*-NN) and support vector machine (SVM) [9][10][11][12][13]; however, they are highly depended on whether the feature set could provide descriptive and discriminative description. Therefore, it is a critical task to have a well-performed feature design so that the classifier could be able to differentiate among different categories precisely. Currently, some advanced computer vision methodologies have been incorporated into nodule imaging analysis. For example, local binary patterns (LBP), speeded up robust features (SURF) and scale-invariant feature transform (SIFT) [1][10][14][15][16] are used to as the feature description for lung nodule.

Normally, the effectiveness of image feature description

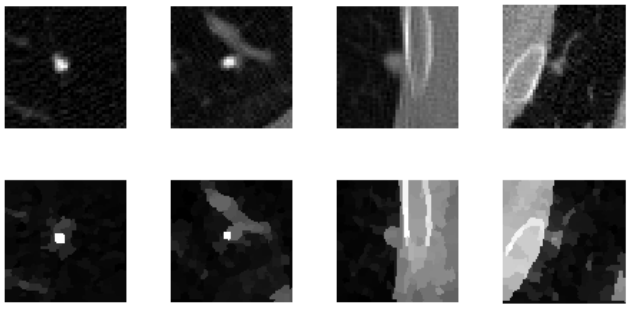

Fig. 2. Example patch division representation of the sample images from the four types of lung nodules. The first row shows the original images and the second one shows the corresponding patch division. The patch is indicated with the same grey level within the local area, which represents certain anatomical structure.

depends on two main factors: distinction and invariance, which means that the descriptor needs to capture the distinctive characteristics and be robust to adapt to the various imaging conditions [1][17]. However, the above techniques mostly emphasize on the nodule structures, restricting their ability to differentiate the intra-type nodules due to overlapping feature spaces of the nodules from different categories [10]. In addition, lung nodule is so complicated with various anatomical structures that those techniques would introduce large degree of unnecessary feature variations when concerning too many image details. Hence, the emphasis of feature design for lung nodule classification should be twofold. Firstly, the surrounding context information should be incorporated to a larger extent for capturing a more comprehensive description of the lung nodule image, since the neighbouring anatomical structures provide important cues in differentiating various lung nodules. Secondly, trivial context details should be eliminated in order to highlight the major anatomical structures.

While lots of works have been reported in segmentation and detection of lung nodules [18][19], there are only few works in analyzing the context information. A stratified learning approach was proposed for lung nodule detection by firstly classifying the various anatomical structures around the nodule [20]. However, this approach captures too many details since there is no need to accurate label each pixel. With a similar aim of the first step of our proposed method that parses the anatomical context information before classification, a graph-based pixel labeling method was introduced in [21], but the segmentation process was over-complicated. Furthermore, we believe that better performance would be achieved by analyzing the labeling result according to the characteristics of lung nodules instead of adopting the general methodologies (SIFT was used in [21]).

B. Outline of the proposed method

In light of above, we propose a new feature description for the lung nodule image, which is used to automatically classify the various lung nodules. The contributions of the proposed feature design are twofold. First, a superpixel labeling is conducted to label the context into foreground and background based on the patch division that groups related pixels together to represent certain anatomical structure. Instead of labeling the pixels directly, the proposed patch-based approach could provide a preprocessing to incorporate local spatial information and reduce spurious labeling. Second, a new feature descriptor, called context curve, is calculated according to the obtained labeling result by capturing the variation of foreground pixels. The proposed context curve focuses on describing the major common anatomical structures of intra-type nodules, and provides an efficient solution to handle the rotation-invariant problem.

Then, the classification is conducted with SVM classifier based on the proposed feature descriptor. The evaluation is carried out on a publicly available database, with lung nodule centroids annotated by the positions. The quantitative comparisons among various approaches indicate the promising performance of the proposed method.

II. METHOD

A. Patch division

A patch-based approach is based on partitioning the image into an orderless collection of smaller patches [22], among which each individual patch depicts a single anatomical structure. For example, Fig.2 shows a patch-based representation of the example images from the four types of lung nodules. Patch division provides an efficient approach to capture the local details in order to better represent the heterogeneous structures other than the overall description of the image, especially for the lung nodule image that contains complicated anatomical structures.

Instead of forming the division in a rigid manner, i.e. dividing the image into patches with predefined shape and size such as square patches [23][24] or circular sectors [7][25], which would unavoidably group different anatomical structures together, the formulation of patches should be adaptive to the local information. Based on our visual analysis of lung nodule images, it is observed that pixels with the similar intensity within the local area usually represent the same anatomical structure. Therefore, we design an adaptive patch division method formulating superpixels using an improved quick shift clustering method [26]. Formally, denoting an image as $I = \{p_i : i = 1, ..., N\}$ with N pixels. The outcome of superpixel formulation represents the image I as $I_{sp} = \{sp_j : j = 1, ..., M\}$ with M superpixels ($M \ll N$). The pixels with the same superpixel value sp are grouped together as one patch pat.

Specifically, the quick shift clustering is applied to the amplified image due to the small size of lung nodule (the diameter is only about 30mm [3]). In the original lung nodule image, only a few pixels could represent a certain structure so that direct use of quick shift is of high possibility in clustering trans-regional pixels together, leading to a poor division, as illustrated in Fig.3. For our proposed scheme, the image is firstly amplified with nearest neighbour interpolation [27]. Quad-amplification proved to generate the best performance in our experiments. Then, the quick shift clustering is applied to the amplified image to formulate the superpixels. Finally, the downsampling step is employed to restore the superpixel image to the original size. The clusters are thus the desired image patches. The illustration of the proposed image division on sample images are shown in Fig.3.

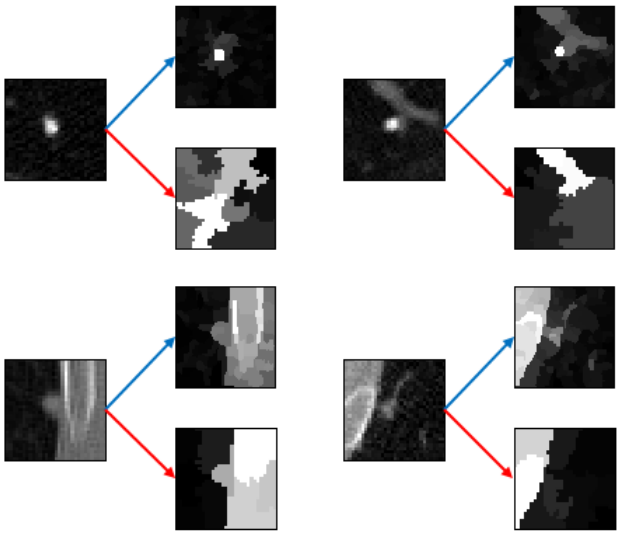

Fig. 3. The patch division of sample images using the proposed scheme (blue arrows) and direct use of quick shift on the original images (red arrows). The direct use of quick shift tends to incorporate trans-regional pixels, so it is hard to capture the context information precisely.

B. Superpixel labeling

While the patch-based image presentation through superpixel formulation could better describe the context information through incorporating the local information and reducing spurious labeling, it is still hard to classify the images based on patch division outcomes. Firstly, although the proposed patch division could depict the context by identifying various anatomical structures, the correlations of them in different images are difficult to be established for the aim of classification. In addition, the patch division still captures too many unnecessary details except for the major anatomical structures such as the vessels and pleural surfaces. Therefore, we would like to further perform a superpixel labeling differentiating each pixel into foreground or background in order to handle the above issues.

Separating the foreground (i.e. nodule, vessels and pleural surfaces) from the background (i.e. parenchyma and trivial detail tissues) is to extract the common characteristics among the intra-type nodules and eliminate the some unnecessary details. In particular, the desirable anatomical structures of the foreground for each type of nodules, which are essential for type decision, is shown in Tab.I. The sample labeling results for the example images are shown in Fig.4.

As for the aim of lung nodule classification, which does not require precise labeling that usually needs over-complicated segmentation, we could easily achieve a desirable outcome based on the patch division. Specifically, for the superpixel representation of image I, i.e. $I_{sp} = \{sp_j : j = 1, ..., M\}$, each superpixel sp is firstly labeled as 1 (foreground) or 0 (background). Then, the labeling result of images I is thus obtained according to the corresponding superpixel labeling. Through our experiments, we found that the thresholding algorithm using Otsu method on I_{sp} can deliver better performance.

TABLE I. APPROXIMATE ANATOMICAL CONTEXT OF LEVEL PATCH FOR EACH TYPE

Type	W	V	J	P
Foreground	nodule	nodule	nodule	nodule
		vessel	pleura	pleura

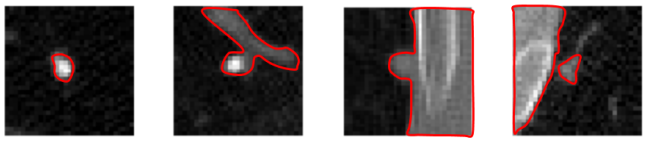

Fig. 4. The illustration of foreground identification of the sample images from the four types of lung nodules, encircled in red. W: nodule; V: nodule + vessel; J: nodule + pleural surface; P: nodule + pleural surface.

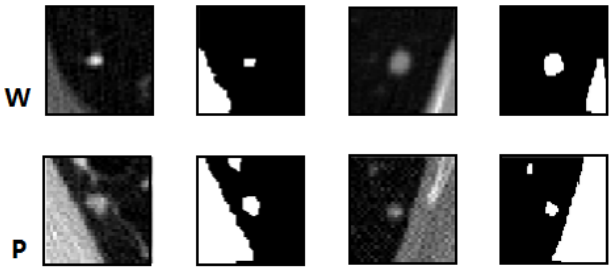

Fig. 5. Sample images for type W and P nodules and the corresponding superpixel results.

C. Context curve construction

Next, the description of the lung nodule image is extracted in terms of feature vector based on the superpixel labeling result. Firstly, the feature descriptor should be able to quantitatively describe both the nodule and the surrounding anatomical structures in order to incorporate the context information. Also, it should capture the common characteristics among intra-type lung nodules, in spite of the various image variances. In particular, the feature design should be rotation invariant to accommodate the diversity of appearance within a certain nodule category. Taking type P as example, as shown in Fig.5, the relative positions of pleural surfaces regarding to the centroids of lung nodules are not coincided. In addition, the feature vector should have the ability to clearly differentiate inter-type nodules since the nodules from different categories sometimes might be quite similar. For example, the superpixel labeling results of type W nodules might be similar to those from type P after extracting the main foreground structures if these type W nodules are near the pleural surfaces, as shown in Fig.5.

Considering these points, a context curve is thus calculated for each lung nodule image based on the superpixel labeling result. Formally, for image I, superpixel labeling output is firstly partitioned into circular sections $SEC = \{sec_k : k = 1, ..., K\}$ with K sections. Then, the foreground ratio $FR = \{fr_k : k = 1, ..., K\}$ is computed for each section sec_k, i.e.

$$fr_k = foreground(sec_k)/all(sec_k) \quad (1)$$

where $foreground$ and all are the numbers of foreground and all pixels respectively. The final feature vector $F(I) =$

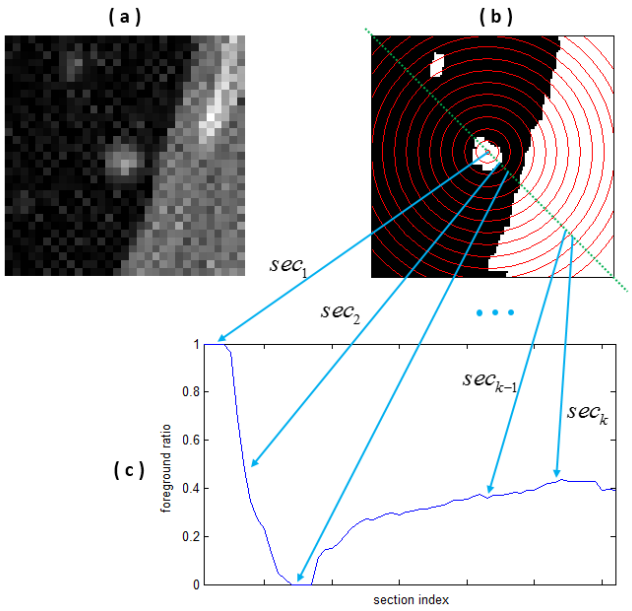

Fig. 6. The procedure of calculation of context curve. (a) The original sample CT slide. (b) The superpixel labeling result with the circular partition. (c) The context curve. The red concentric circles indicate the context partition based on the distance of each pixel to centroid of the lung nodule. The light blue arrows indicate the foreground ratio for each section.

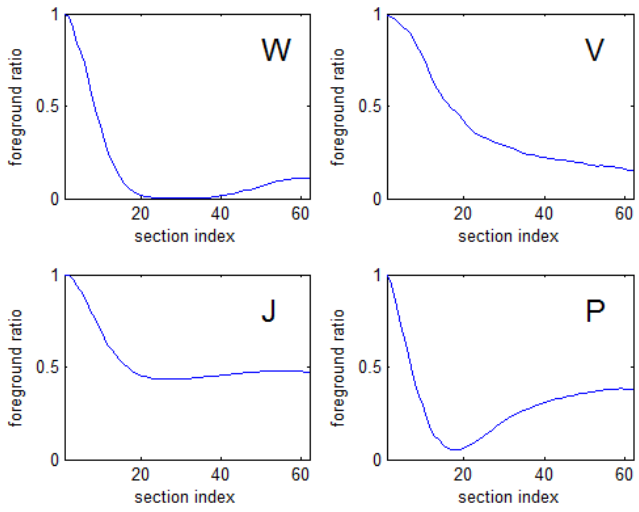

Fig. 7. The templates of context curves for the four types of the lung nodules, which are computed according to the average foreground ratio of the same level sections throughout the whole dataset.

$\{f_k = fr_k : k = 1, ..., K\}$ is obtained by combining the foreground ratios of all sections from inside to outside. The overall procedure is illustrated in Fig.6.

The circular partition is obtained by grouping the pixels that have the same distance to the centroid of lung nodule together. The total number of sections, K, is determined by the size of image, which is the radius of the last concentric circle that reaches the edge of the image. Due to the small size of the lung nodule, the superpixel labeling result is also amplified as introduced in Section II.A to better describe the foreground. In our experiments, a sub-window of 31×31 was cropped from each image slide with the nodule in the center (introduced in Section V in detail) and quad-amplification was adopted; thus, K was settled as 62. In addition, although the annotated nodule centroid given in the dataset can be directly used as the centroid of the lung nodule, we choose to refine it since the annotated positions deviate from the actual geometric centroids for some slides. The centroid of the nodule is finally fixed at the location that makes the inside sections with $fs = 1$ as many as possible.

Next, for each section sec, the foreground ratio fr is calculated by counting the pixels belonging to the foreground. While the inside several sections depict the nodule, whose fr are around 1, the outside ones describe the context information, whose fr are diverse upon various context structures. For example, foreground ratio of the sections describing the pleural surface usually ranges from 0.3 to 0.5, and describing the parenchyma are normally around 0.

Finally, the context curve is obtained by concatenating all foreground ratios from the inside to outside. Since context curve focuses on depicting the major foreground structures for different types of nodules, it can better capture the common characteristics of intra-type nodules. Also, context curve is based on the two pre-stages, i.e. patch division and superpixel labeling, which have already eliminated the trans-regional details, so it can make distinct differentiations among inter-type nodules. In addition, the calculation of foreground ratio is independent on the relative positions, thus the context curve can accommodate the rotation variant. The general trend of context curve for each type of lung nodule follows the templates shown in Fig.7.

D. Classification based on the context curve

The last stage of the proposed method is to classify the lung nodules into the given four types, i.e. W, V, J and P, according to the extracted context curves. SVM classifier is used to conduct the classification. Specifically, a four-type SVM is trained with polynomial kernel by C-SVC from [28], and the probability estimates upon the different types are predicted with the obtained SVM model, which is used to classify the feature descriptors into four categories

III. Experiments and Results

A. Dataset

The experiments were conducted on the publicly available Early Lung Cancer Action Program (ELCAP) [29] database, which contains 50 sets of low-dose CT lung scans with 379 unduplicated lung nodules. The centroids of nodules are approximately indicated by the annotated locations. The nodules are further classified into well-circumscribed (W-15%), vascularized (V-16%), juxta-pleural (J-30%) and pleural-tail (P-39%) by an expert reader of the images.

During the preprocessing stage, a sub-window of 31×31 pixels was cropped for each nodule with the annotated centroid appearing in the center. This is similar to the handling in [10][15][21] for focusing on the small size lung nodule.

The percentages of training dataset were randomly selected from 10% to 90% for each of the four types, and the remaining

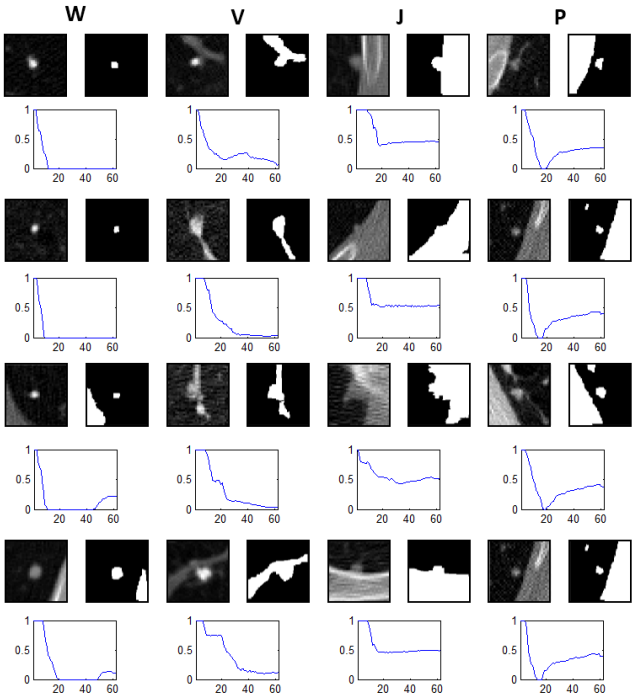

Fig. 8. Superpixel labeling outputs and context curves of the example images for each type: W, V, J and P respectively. For each of these images, the left above indicates the original CT slides, the right above indicates the superpixel labeling results with white for foreground and black for background, and the below indicates the context curves.

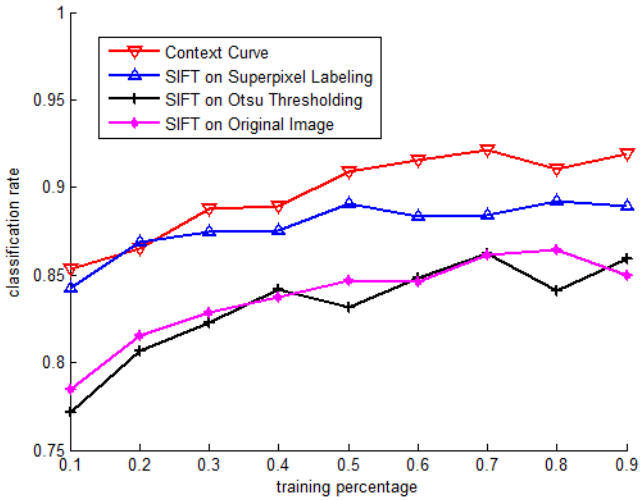

Fig. 9. The comparison of the classification rates upon various training percentages among the given four approaches: context curve, SIFT based on superpixel labeling, SIFT based on Otsu thresholding, and raw SIFT descriptor. Different feature descriptors are extracted to describe the nodules and the same SVM classifier is used to categorize them into four types.

were used for testing. The selection of various sizes of training datasets is to make sure that the proposed method can work even in adverse circumstances. The performance is quantitatively evaluated by computing the overall classification rate, i.e. the ratio of correctly classified nodules out of the whole within the testing dataset.

B. Results

Examples of superpixel labeling results and context curves on the four types of lung nodules are shown in Fig.8. Based on our visual inspection, the overall results suggest a good labeling performance by using the proposed patch division and superpixel labeling, which can better capture the major anatomical structures for various types of nodules. Also, the derived context curves can well depict the labeling results following the templates described in Section II.C for different categories.

In order to show the advantages of superpixel labeling and context curve, Fig.9 shows the comparisons among the following approaches, all of which use the same SVM classifier but extract different feature descriptors: the proposed context curve descriptor, SIFT descriptor based on the proposed superpixel labeling, SIFT descriptor based on Otsu thresholding, and the raw SIFT descriptor. As for the second and third approaches, SIFT descriptor is extracted at the centroid of the processed image respectively. The last approach extracts the SIFT descriptor from the original lung nodule image.

Firstly, the classification rate of superpixel labeling based approach is with improvement, about 4.5% more of the images are correctly classified, over the raw SIFT approach, suggesting that identifying the foreground structures can better describe the lung nodule images for the aim of classification than directly utilizing the original images. Usually, the original images contain unnecessary detail anatomical structures which could influence the extraction of major information. In addition, extracting SIFT descriptor based on Otsu thresholding obtains a quite similar result with raw SIFT approach, which is lower than the superpixel labeling approach as well, indicating the advantage of the proposed patch division that is more suitable for foreground identification. Although the SIFT based on superpixel labeling obtains a promising performance, more nodules are correctly classified with the proposed context curve descriptor. It shows that the context curve, which concerns both the nodule structure and surrounding context, can better provide the distinctive description according to the characteristics of various types of nodules.

The evaluation for the proposed method regarding to state of the art methods for lung nodule classification is shown in Fig.10. The comparisons are conducted among the following methods: the proposed method, the weighed clique percolation method (CPMw) upon SVM probability estimates [10], SVM classification upon SIFT descriptor [10], linear discriminant analysis (LDA) upon SIFT descriptor [15], principle component analysis (PCA) upon SIFT descriptor [15] and the standard k-NN upon SIFT descriptor. Fig.10 shows the average classification rate across all training percentages (10%-90%) for each of these methods.

The last three approaches achieve relatively lower classification rates, around 78% lung nodules correctly classified. Especially for LDA and PCA upon SIFT descriptors, their less promising performances are due to fact that they are not effective enough when only a small percentage of dataset is involved for training, as illustrated in [15]. However, as for the proposed method, it is less dependent on the size of training dataset, which can be seen in Fig.9. The distribution

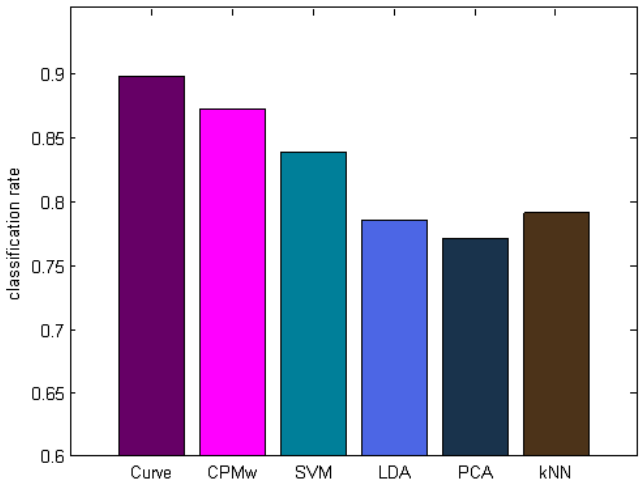

Fig. 10. The average classification rates comparing various methods: proposed method, CPMw upon SVM probability estimates, SVM classification upon SIFT descriptor, LDA upon SIFT descriptor, PCA upon SIFT descriptor, and k-NN upon SIFT descriptor.

of classification rate given various training percentages is relatively stable. The first three ones obtain better results among all control approaches. CPMw was used to identify the overlapping nodules in [10] in order to improve the classification; however, without concerning such issue, the proposed method still achieves better result, with 3% more of nodules correctly classified. Overall, it is apparent that our proposed method results in the best performance, suggesting its promising ability for lung nodule classification.

IV. Conclusion

In this paper, we propose a novel method for lung nodule image classification, regarding to the four types, i.e. well-circumscribed, juxta-vascular, juxta-pleural and pleural-tail. Firstly, the lung nodule image is parsed to identify the major anatomical context information based on the proposed patch division and superpixel labeling. Then, a new feature descriptor, context curve, is designed to describe the processed image quantitatively according to the characteristics of each type of lung nodules. Providing discriminative descriptions of stage of the art lung nodules, the proposed feature can be used to achieve better classification result. Our method is evaluated using ELCAP database, and the comparisons with various methods demonstrate its high performance on lung nodule classification.

References

[1] A. Farag, A. Ali, J. Graham, and et al., "Evaluation of geometric feature descriptors for detection and classification of lung nodules in low dose ct scans of the chest," in *Proc. ISBI*, 2011, pp. 169–172.

[2] J. J. Erasmus, J. E. Connolly, and et al., "Solitary pulmonary nodules: Part i. morphologic evaluation for differentiation of benign and malignant lesions1," *Radiographics*, vol. 20, no. 1, pp. 43–58, 2000.

[3] B. B. Tan, K. R. Flaherty, E. A. Kazerooni, and et al., "The solitary pulmonary nodule," *CHEST Journal*, vol. 123, no. 1, pp. 89–96, 2003.

[4] D. M. Xu and et al., "Smooth or attached solid indeterminate nodules detected at baseline ct screening in the nelson study: Cancer risk during 1 year of follow-up," *Radiology*, vol. 250, no. 1, pp. 264–272, 2009.

[5] S. Diciotti, G. Picozzi, M. Falchini, and et al., "3-d segmentation algorithm of small lung nodules in spiral ct images," *IEEE Trans. Information Technology in Biomedicine*, vol. 12, no. 1, pp. 7–19, 2008.

[6] B. Zhao, "Automatic detection of small lung nodules on ct utilizing a local density maximum algorithm," *Journal of Applied Clinical Medical Physics*, vol. 4, no. 3, pp. 248–260, 2003.

[7] D. Unay and A. Ekin, "Dementia diagnosis using similar and dissimilar retrieval items," in *Proc. ISBI*, 2011, pp. 1889–1892.

[8] Y. Song, W. Cai, J. Kim, and D. Feng, "A multi-stage discriminative model for tumor and lymph node detection in thoracic images," *IEEE Trans. Medical Imaging*, vol. 31, no. 5, pp. 1061–1075, 2012.

[9] S. L. A. Lee, A. Z. Kouzani, and E. J. Hu, "Automated detection of lung nodules in computed tomography images: a review," *Machine vision and applications*, vol. 23, no. 1, pp. 151–163, 2012.

[10] F. Zhang, W. Cai, and et al., "Overlapping node discovery for improving classification of lung nodules," in *Proc. EMBC*, 2013, pp. 5461–5464.

[11] L. Srensen, S. B. Shaker, and M. De Bruijne, "Quantitative analysis of pulmonary emphysema using local binary patterns," *IEEE Trans. Medical Imaging*, vol. 29, no. 2, pp. 559–569, 2010.

[12] C. Jacobs, C. I. Snchez, S. C. Saur, and et al., "Computer-aided detection of ground glass nodules in thoracic ct images using shape, intensity and context features," in *MICCAI LNCS*, 2011, pp. 207–214.

[13] Y. Song, W. Cai, and et al., "Thoracic abnormality detection with data adaptive structure estimation," in *MICCAI LNCS*, 2012, pp. 74–81.

[14] A. Farag, A. Ali, J. Graham, and et al., "Feature-based lung nodule classification," in *Advances in Visual Computing*, 2010, pp. 79–88.

[15] A. Farag, S. Elhabian, J. Graham, A. Farag, and R. Falk, "Toward precise pulmonary nodule descriptors for nodule type classification," in *MICCAI LNCS*, vol. 13, no. 3, 2010, pp. 626–633.

[16] Y. Song, W. Cai, Y. Zhou, and D. Feng, "Feature-based image patch approximation for lung tissue classification," *IEEE Trans. Medical Imaging*, vol. 32, no. 4, pp. 797–808, 2013.

[17] Y. Song and et al., "Discriminative data transform for image feature extraction and classification," in *MICCAI LNCS*, 2013.

[18] I. Sluimer, A. Schilham, M. Prokop, and B. van Ginneken, "Computer analysis of computed tomography scans of the lung: a survey," *IEEE Trans. Medical Imaging*, vol. 25, no. 4, pp. 385–405, 2006.

[19] Y. Song, W. Cai, and et al., "Discriminative pathological context detection in thoracic images based on multi-level inference," in *MICCAI LNCS*, 2011, pp. 191–198.

[20] D. Wu, L. Lu, J. Bi, Y. Shinagawa, K. Boyer, A. Krishnan, and M. Salganicoff, "Stratified learning of local anatomical context for lung nodules in ct images," in *Proc. CVPR*, 2010, pp. 2791–2798.

[21] Y. Song, W. Cai, and et al., "Location classification of lung nodules with optimized graph construction," in *Proc. ISBI*, 2012, pp. 1439–1442.

[22] S. O'Hara and B. A. Draper, "Introduction to the bag of features paradigm for image classification and retrieval," *Computer Vision and Pattern Recognition*, 2011.

[23] J. Galaro and et al., "An integrated texton and bag of words classifier for identifying anaplastic medulloblastomas," in *Proc. EMBC*, 2011, pp. 3443–3446.

[24] A. Cruz-Roa, F. Gonzlez, and et al., "A visual latent semantic approach for automatic analysis and interpretation of anaplastic medulloblastoma virtual slides," in *MICCAI LNCS*, vol. 7510, 2012, pp. 157–164.

[25] Y. Song, W. Cai, Y. Zhou, L. Wen, and D. Feng, "Pathology-centric medical image retrieval with hierarchical contextual spatial descriptor," in *Proc. ISBI*, 2013, pp. 202–205.

[26] A. Vedaldi and S. Soatto, "Quick shift and kernel methods for mode seeking," in *Proc. ECCV*, 2008, pp. 705–718.

[27] J. W. Hwang and H. S. Lee, "Adaptive image interpolation based on local gradient features," *IEEE Signal Processing Letters*, vol. 11, no. 3, pp. 359–362, 2004.

[28] C.-C. Chang and C.-J. Lin, "Libsvm: a library for support vector machines," *ACM Trans. TIST*, vol. 2, no. 3, p. 27, 2011.

[29] P. F. Felzenszwalb, R. B. Girshick, D. McAllester, and D. Ramanan, "Object detection with discriminatively trained part-based models," *IEEE Trans. Pattern Analysis and Machine Intelligence*, vol. 32, no. 9, pp. 1627–1645, 2010.